

Dibenzo[*b, e*]-7,7,8,8-tetraneopentyl- and dibenzo[*b, e*]-7,7,8,8-tetraisopropyl-7,8-disilabicyclo[2.2.2]octa-2,5-dienes: interaction with tetracyanoethylene and transition metal chlorides

Soichiro Kyushin^a, Masanobu Ikarugi^a, Kazutoshi Takatsuna^a, Midori Goto^b,
Hideyuki Matsumoto^{a,*}

^a Department of Applied Chemistry, Faculty of Engineering, Gunma University, Kiryu, Gunma 376, Japan

^b National Institute of Materials and Chemical Research, Tsukuba, Ibaraki 305, Japan

Received 28 June 1995; in revised form 30 August 1995

Abstract

Dibenzo[*b, e*]-7,7,8,8-tetraalkyl-7,8-disilabicyclo[2.2.2]octa-2,5-dienes (**1**: R = ^tBuCH₂; **2**: R = ⁱPr) were prepared by the reaction of ClR₂SiSiR₂Cl with lithium anthracenide in 1,2-dimethoxyethane (DME) at room temperature. The structure of **1** was determined by X-ray crystallography. Crystal data for **1**: monoclinic, *C*2/*c*, *a* = 12.941(2), *b* = 14.601(1), *c* = 35.109(6) Å, β = 94.957(7)°, *V* = 6609(2) Å³, *Z* = 8, *R* = 0.048, *R*_w = 0.053 for 4037 reflections. Compounds **1** and **2** show the bathochromic shift of ¹L_a and ¹L_b bands in UV spectra and exhibit considerably low oxidation potentials due to effective σ–π conjugation. Compounds **1** and **2** form charge-transfer complexes with tetracyanoethylene (TCNE). In the case of **1**, the charge-transfer complex (**1**: TCNE = 2:1) could be isolated as crystals and the structure was determined by X-ray crystallography. Crystal data for the **1**–TCNE complex: monoclinic, *C*2/*c*, *a* = 10.267(2), *b* = 36.077(4), *c* = 20.022(4) Å, β = 100.680(8)°, *V* = 7288(2) Å³, *Z* = 4, *R* = 0.045, *R*_w = 0.077 for 4120 reflections. The action of transition metal chlorides on **2** resulted in [4 + 2] cycloreversion to form ClⁱPr₂SiSiⁱPr₂Cl and anthracene.

Keywords: Silane; Group 14; σ–π conjugation; Charge transfer; Crystal structure; Cycloreversion

1. Introduction

7,7,8,8-tetraalkyl-7,8-disilabicyclo[2.2.2]octa-2,5-dienes are fascinating molecules because they are known to produce transient or nearly stable tetraalkyldisilenes on photolysis and thermolysis [1,2]. Quite recently, novel [4 + 2] cycloreversion of 2,3-disilabicyclo[2.2.2]octa-5,7-dienes induced by electron-transfer was published by Nakadaira et al. [3], who found that photolysis of 1-phenyl-2,2,3,3-tetramethyl-2,3-disilabicyclo[2.2.2]octa-5,7-diene with 9,10-dicyanoanthracene as a sensitizer yielded biphenyl as a tetramethyldisilene extrusion product. This publication also described that addition of an equimolar amount of tetracyanoethylene (TCNE) to dibenzo[*b, e*]-7,7,8,8-tetramethyl-7,8-

disilabicyclo[2.2.2]octa-2,5-diene (**3**) resulted in the formation of dibenzo[*b, e*]-7,7,8,8-tetracyanobicyclo[2.2.2]octa-2,5-diene (a TCNE adduct of anthracene) via a charge-transfer complex. However, in this example, isolation of the charge-transfer complex of **3** with TCNE was not reported.

Recently, we have been interested in polycyclocarbopolysilanes in which strained Si–C or Si–Si bonds interact with π systems. In preceding papers [4], we reported the synthesis, molecular structure and charge-transfer complexes of *cis*-dibenzo[*c, h*]-1,6-disilabicyclo[4.4.0]deca-3,8-dienes and bi(benzo[*c*]silacyclopent-3-en-1-yl)s. In the present work, dibenzo[*b, e*]-7,7,8,8-tetraalkyl-7,8-disilabicyclo[2.2.2]octa-2,5-dienes were chosen as target molecules because they may possess unique properties due to strong σ–π interaction. Herein we present the following new information: (1) the X-ray structure of dibenzo[*b, e*]-7,7,8,8-tetraneopentyl-7,8-disilabicyclo[2.2.2]octa-2,5-diene (**1**);

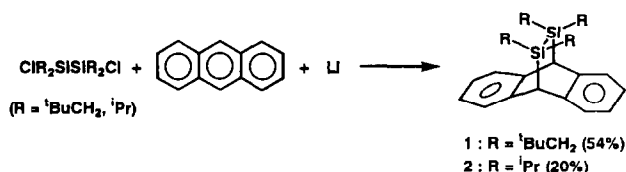
* Corresponding author.

(2) isolation and the X-ray crystal structure of the charge-transfer complex of **1** with TCNE; (3) the action of transition metal chlorides on dibenzo[*b,e*]-7,7,8,8-tetraisopropyl-7,8-disilabicyclo[2.2.2]octa-2,5-diene (**2**) leading to [4 + 2] cycloreversion. Results on photochemical [4 + 2] cycloreversion of **2** have been reported previously [5].

2. Results and discussion

2.1. Synthesis of **1** and **2**

Compounds **1** and **2** were prepared by the reaction of 1,2-dichloro-1,1,2,2-tetraalkyldisilanes with lithium anthracenide according to Roark and Peddle's method [2a]. The yield of the compounds depends upon reaction conditions; optimum conditions involve treatment of 1,2-dichloro-1,1,2,2-tetraalkyldisilanes with 2 equiv. of anthracene and 2.2 equiv. of lithium in 1,2-dimethoxyethane (DME) at 20°C (Table 1). Under these conditions, **1** and **2** were isolated in 54 and 21% yields respectively. These compounds are infinitely stable in air at room temperature, indicating that both neopentyl and isopropyl groups can serve as effective blockades against external attack.



2.2. Structure of **1**

Recently, Sekiguchi et al. [2i] reported the X-ray structure of 7,7,8,8-tetramethyl-7,8-disilabicyclo[2.2.2]octa-2,5-diene (**4**). However, crystallographic data have not yet been available for the dibenzo[*b,e*]-7,7,8,8-tetraalkyl-7,8-disilabicyclo[2.2.2]octa-2,5-diene system. We have thus carried out the X-ray analysis of **1**. The

Table 1
Comparison of reaction conditions in the synthesis of **2**

Run	Molar ratio of Cl ⁱ Pr ₂ SiSi ⁱ Pr ₂ Cl: anthracene:Li	Solvent	Temperature (°C)	Yield of 2 (%) ^a
1	1:1:2.2	DME	20	25
2	1:2:2.2	DME	20	36
3	1:2:2.2	DME	-77	< 1
4	1:2:4.5	DME	20	23
5	1:2:2.2	THF	20	23

^a Determined by GLC.

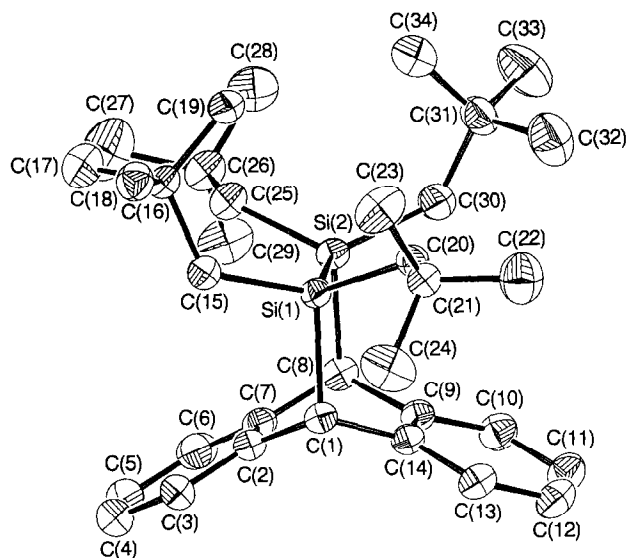


Fig. 1. ORTEP drawing of **1**. Thermal ellipsoids are drawn at the 30% probability level.

molecular structure of **1** is shown in Fig. 1. Crystallographic data, positional parameters and selected bond distances and angles are summarized in Tables 2–4. Several structural features were noted for **1**. The Si–Si bond length (2.389(2) Å) is somewhat longer than that of **4** (2.363(2) Å). The Si–C bonds (Si(1)–C(1): 1.938(6) Å and Si(2)–C(8): 1.943(6) Å) are elongated compared with that of **4** (1.919 Å). The elongation of the Si–Si and Si–C bonds may be a result of greater steric repulsion caused by the bulky neopentyl groups. The bond angles around the bridged Si atoms (Si(2)–Si(1)–C(1): 96.0(2)° and Si(1)–Si(2)–C(8): 95.2(2)°) are highly contracted similarly to the value of 96.3° found in **4**. The Si–Si–C(neopentyl) angles range from 107.5(2)° to 122.7(2)°, again indicating the steric repulsion between the neopentyl groups.

In benzyldisilane derivatives, it is known that σ – π conjugation operates most effectively when a benzylic Si–C bond and *p* orbitals of benzene rings are coplanar [6]. In compound **1**, fairly good planarity is found. Thus, the dihedral angles between the benzylic Si–C bonds and the *p* orbitals of the benzene rings are 17.4° (Si(1)–C(1) and C(2)–C(7)), 18.1° (Si(1)–C(1) and C(9)–C(14)), 19.1° (Si(2)–C(8) and C(2)–C(7)) and 14.3° (Si(2)–C(8) and C(9)–C(14)) with an average of 17.2°. Therefore, effective σ – π conjugation is expected to operate in compounds **1** and **2**.

The X-ray structure of **1** illustrated in Fig. 1 explains clearly the NOESY spectrum of **1**. As shown in Fig. 2, NOE peaks are observed between CH₃ and H^a, CH₃ and H^b, and H^a and H^b; the cross peak intensities are comparable. This result is consistent with the short distances between CH₃ and H^a, CH₃ and H^b, and H^a and H^b (2.41, 2.21 and 2.39 Å respectively). Weak

NOE cross peaks between CH₂ and H^a, CH₂ and H^b and between CH₃ and H^c are also found.

2.3. Electronic properties of **1** and **2**

Electrochemical behavior of **1** and **2** was investigated by cyclic voltammetry. These compounds undergo irreversible oxidation, and oxidation potentials (E_p^{ox}) for both the compounds are similar and considerably low (1.17 V vs. SCE in acetonitrile), indicating that the

highest occupied molecular orbital (HOMO) of each compound is destabilized due to the effective σ - π conjugation mentioned above. The value of 1.17 V is noticeably smaller than those of *cis*-dibenzo[*c,h*]-1,6-diisopropyl-1,6-disilabicyclo[4.4.0]deca-3,8-diene (**5**: $E_p^{ox} = 1.35$ V vs. SCE in acetonitrile), reflecting the difference in the dihedral angles between the benzylic Si-C bonds and the *p* orbitals of the benzene rings (**5**: 24.1°–29.2°) [4].

UV spectra of **1** and **2** are shown in Fig. 3. In these

Table 2
Summary of crystal data, data collection and refinement

	1	1-TCNE
<i>Crystal data</i>		
Formula	C ₃₄ H ₅₄ Si ₂	2C ₃₄ H ₅₄ Si ₂ · C ₆ N ₄
Molecular weight	518.98	1166.05
Crystal description	Colorless prisms	Green plates
Crystal size (mm)	0.5 × 0.5 × 0.2	0.5 × 0.15 × 0.8
Crystal system	Monoclinic	Monoclinic
Space group	C2/c	C2/c
<i>a</i> (Å)	12.941(2)	10.268(2)
<i>b</i> (Å)	14.601(1)	36.077(4)
<i>c</i> (Å)	35.109(6)	20.022(4)
β (°)	94.957(8)	100.680(8)
<i>V</i> (Å ³)	6609(2)	7288(2)
<i>Z</i>	8	4
D_{measd} (g cm ⁻³)	1.044	1.045
D_{calcd} (g cm ⁻³)	1.043	1.063
<i>Data collection</i>		
Diffractometer	Enraf-Nonius CAD-4	Enraf-Nonius CAD-4
Radiation (λ (Å))	Cu K α (1.5418)	Cu K α (1.5418)
μ (cm ⁻¹)	10.67	10.56
Absorption correction	Empirical	Empirical
T_{min}	0.946	0.756
T_{max}	0.997	1.000
Variation of standards	-1.1%	None
2 θ range (°)	7–130	6–120
Range of <i>h</i>	0 to 15	0 to 11
<i>k</i>	0 to 17	0 to 40
<i>l</i>	-41 to 41	-22 to 22
Scan type	ω - θ	ω -2 θ
Scan width (°)	0.8 + 0.15 tan θ	0.7 + 0.15 tan θ
No. of reflections measured	5626	5766
No. of independent reflections	5626	5108
No. of observed reflections ($ F_o \geq 3\sigma(F_o)$)	4037	4120
<i>Refinement</i>		
<i>R</i>	0.048	0.045
<i>R_w</i>	0.053	0.077
Weighting scheme	$w = 1/[0.00219 F_o ^2 - 0.09781 F_o + 4.96450]$	$w = 1/[28.00(\sin \theta/\lambda)^2 - 493.0 \sin \theta/\lambda + 111.7]$
<i>S</i>	2.54	4.32
(Δ/σ) _{max}	2.431	1.023
($\Delta\rho$) _{max} (e Å ⁻³)	0.35	0.36
($\Delta\rho$) _{min} (e Å ⁻³)	-0.29	-0.40
No. of parameters	325	586

compounds, the absorption bands of the benzene rings are shifted to a longer wavelength region than that of benzene; the 1L_a band has a shoulder at 239 nm (**1**) and 238 nm (**2**), and the 1L_b band appears at 275 and 282 nm (**1** and **2**) accompanied by a marked increase of extinction coefficients. Such a remarkable bathochromic shift is also explained by effective σ - π conjugation.

2.4. Formation of charge-transfer complexes of **1** and **2** with TCNE and the structure of the **1**-TCNE complex

Upon addition of TCNE to dichloromethane solutions of **1** and **2**, the solutions immediately turned dark green. The UV-visible spectra of the colored solutions show new charge-transfer absorption bands (Fig. 4). The charge-transfer spectra show two absorption maxima at 460 nm (21700 cm^{-1}) and 636 nm (15700 cm^{-1}) in the case of **1** and at 457 nm (21900 cm^{-1})

and 630 nm (15900 cm^{-1}) in the case of **2** [7]. These values are favorably compared with the charge-transfer bands of **5** at 448 nm (22300 cm^{-1}) and 559 nm (17900 cm^{-1}) [4].

It has been reported that **3** reacts with TCNE in dichloromethane at room temperature via a charge-transfer complex [3]. However, the charge-transfer absorption bands of **1** and **2** do not change at room temperature. In the case of **1**, we succeeded in isolating the charge-transfer complex. Slow removal of dichloromethane from a solution of the charge-transfer complex of **1** with TCNE gave dark green crystals quantitatively. The complex was found to be stable up to 175° , while it melts and decomposes above 175°C . In contrast, when the solvent was slowly removed from the dichloromethane solution of **2** and TCNE, the donor and the acceptor were recovered quantitatively.

Although many charge-transfer complexes of

Table 3
Fractional atomic coordinates and equivalent isotropic thermal parameters for **1**

Atom	x	y	z	$B_{\text{eq}}^a (\text{\AA}^2)$
Si(1)	0.1923(1)	0.4949(1)	0.0864(1)	2.94(3)
Si(2)	0.2509(1)	0.4723(1)	0.1521(1)	3.30(4)
C(1)	0.1129(4)	0.6047(4)	0.0942(1)	3.3(1)
C(2)	0.0313(4)	0.5840(4)	0.1213(2)	3.7(2)
C(3)	-0.0744(5)	0.5794(4)	0.1091(2)	4.9(2)
C(4)	-0.1458(6)	0.5629(5)	0.1353(3)	6.1(3)
C(5)	-0.1135(6)	0.5521(5)	0.1732(3)	6.2(3)
C(6)	-0.0092(6)	0.5569(5)	0.1858(2)	5.2(2)
C(7)	0.0651(5)	0.5719(4)	0.1598(2)	3.8(2)
C(8)	0.1798(5)	0.5786(4)	0.1705(2)	3.6(2)
C(9)	0.2213(4)	0.6613(4)	0.1512(2)	3.4(1)
C(10)	0.2914(5)	0.7234(4)	0.1695(2)	4.5(2)
C(11)	0.3239(5)	0.7994(5)	0.1502(2)	5.1(2)
C(12)	0.2873(6)	0.8145(4)	0.1127(2)	5.0(2)
C(13)	0.2197(5)	0.7529(4)	0.0941(2)	4.1(2)
C(14)	0.1865(4)	0.6753(4)	0.1129(2)	3.3(1)
C(15)	0.0920(5)	0.4096(4)	0.0660(2)	4.6(2)
C(16)	0.1135(5)	0.3076(4)	0.0562(2)	3.9(2)
C(17)	0.0514(6)	0.2447(5)	0.0805(2)	5.7(2)
C(18)	0.0763(5)	0.2895(5)	0.0145(2)	4.8(2)
C(19)	0.2279(5)	0.2820(4)	0.0629(2)	4.8(2)
C(20)	0.3003(4)	0.5260(4)	0.0557(2)	3.4(1)
C(21)	0.2879(4)	0.5495(4)	0.0123(2)	3.5(1)
C(22)	0.3802(7)	0.6061(6)	0.0031(2)	6.9(3)
C(23)	0.2884(8)	0.4628(6)	-0.0115(2)	6.6(3)
C(24)	0.1902(7)	0.6026(7)	0.0008(2)	7.1(3)
C(25)	0.1892(5)	0.3630(4)	0.1684(2)	4.2(2)
C(26)	0.1969(6)	0.3232(5)	0.2095(2)	4.7(2)
C(27)	0.1180(9)	0.2456(7)	0.2103(3)	9.4(4)
C(28)	0.3033(7)	0.2832(6)	0.2203(2)	6.9(3)
C(29)	0.1755(8)	0.3958(6)	0.2388(2)	7.1(3)
C(30)	0.3907(5)	0.4904(5)	0.1714(2)	4.9(2)
C(31)	0.4873(5)	0.4437(5)	0.1568(2)	5.1(2)
C(32)	0.5332(7)	0.5064(7)	0.1275(3)	7.8(3)
C(33)	0.5703(7)	0.4327(8)	0.1898(3)	9.1(4)
C(34)	0.4616(7)	0.3534(6)	0.1372(3)	7.8(3)

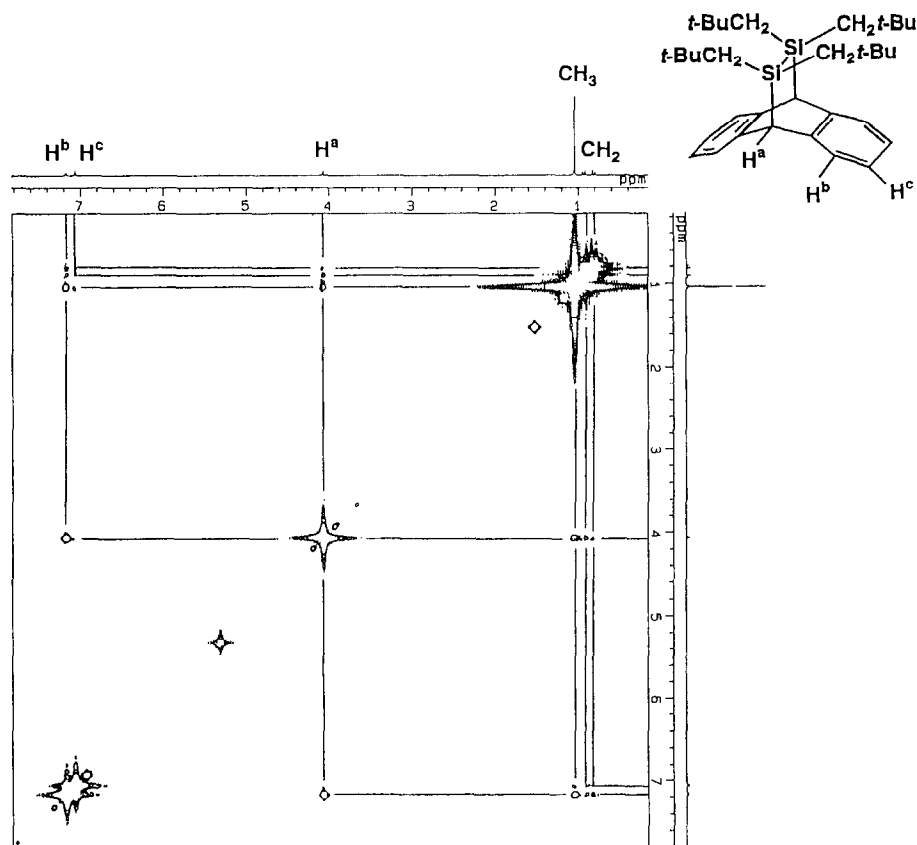
^a Anisotropically refined atoms are given in the form of the equivalent isotropic displacement parameter defined as $B_{\text{eq}} = (4/3)\sum_j \beta_j \mathbf{a}_j \mathbf{a}_j$.

organosilicon compounds are known [8,9], few X-ray structures have been reported [4b,10]. The crystal structure of the **1**-TCNE complex was successfully determined by X-ray crystallography (Fig. 5). Crystallo-

graphic data, positional parameters and selected bond distances and angles are summarized in Tables 2, 5 and 6. The charge-transfer complex contains **1** and TCNE in the ratio 2 : 1. TCNE is surrounded by two molecules of

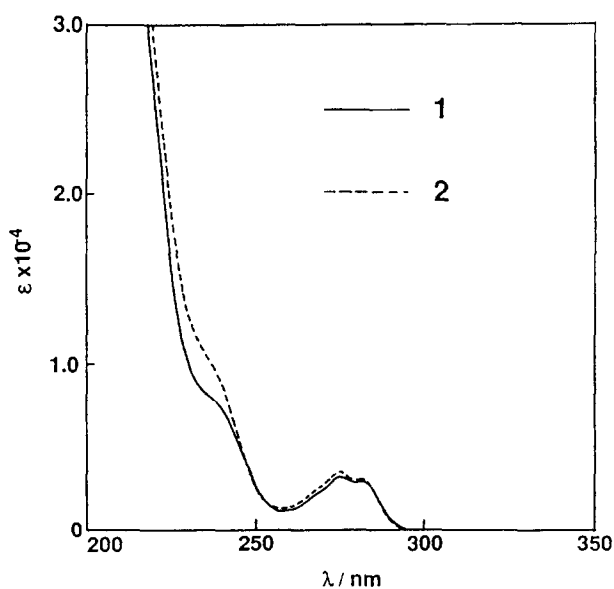
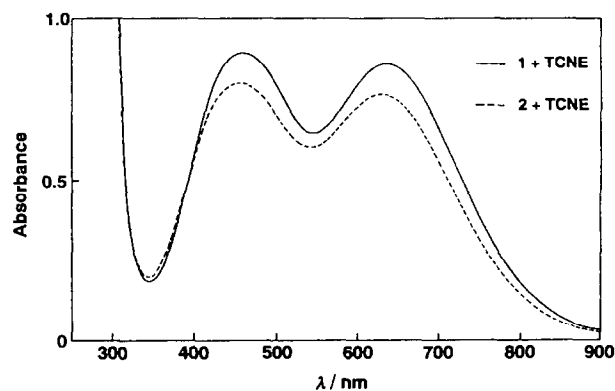
Table 4
Bond distances (Å) and angles (°) for **1**

<i>Bond distances</i>			
Si(1)–Si(2)	2.389(2)	C(11)–C(12)	1.378(10)
Si(1)–C(1)	1.938(6)	C(12)–C(13)	1.379(9)
Si(1)–C(15)	1.894(6)	C(13)–C(14)	1.396(8)
Si(1)–C(20)	1.892(6)	C(15)–C(16)	1.559(8)
Si(2)–C(8)	1.943(6)	C(16)–C(17)	1.528(10)
Si(2)–C(25)	1.895(6)	C(16)–C(18)	1.525(9)
Si(2)–C(30)	1.895(7)	C(16)–C(19)	1.526(9)
C(1)–C(2)	1.510(8)	C(20)–C(21)	1.556(8)
C(1)–C(14)	1.514(7)	C(21)–C(22)	1.511(11)
C(2)–C(3)	1.399(8)	C(21)–C(23)	1.516(10)
C(2)–C(7)	1.397(8)	C(21)–C(24)	1.509(11)
C(3)–C(4)	1.380(12)	C(25)–C(26)	1.552(9)
C(4)–C(5)	1.369(14)	C(26)–C(27)	1.527(13)
C(5)–C(6)	1.385(11)	C(26)–C(28)	1.513(11)
C(6)–C(7)	1.400(10)	C(26)–C(29)	1.519(11)
C(7)–C(8)	1.502(8)	C(30)–C(31)	1.549(10)
C(8)–C(9)	1.506(8)	C(31)–C(32)	1.534(13)
C(9)–C(10)	1.399(8)	C(31)–C(33)	1.519(12)
C(9)–C(14)	1.395(7)	C(31)–C(34)	1.513(12)
C(10)–C(11)	1.384(10)		
<i>Bond angles</i>			
Si(2)–Si(1)–C(1)	96.0(2)	C(11)–C(12)–C(13)	119.9(6)
Si(2)–Si(1)–C(15)	115.1(2)	C(12)–C(13)–C(14)	121.0(6)
Si(2)–Si(1)–C(20)	113.2(2)	C(1)–C(14)–C(9)	117.1(5)
C(1)–Si(1)–C(15)	104.1(3)	C(1)–C(14)–C(13)	123.7(5)
C(1)–Si(1)–C(20)	108.0(2)	C(9)–C(14)–C(13)	119.2(5)
C(15)–Si(1)–C(20)	117.4(3)	Si(1)–C(15)–C(16)	125.6(4)
Si(1)–Si(2)–C(8)	95.2(2)	C(15)–C(16)–C(17)	109.7(5)
Si(1)–Si(2)–C(25)	107.5(2)	C(15)–C(16)–C(18)	109.3(5)
Si(1)–Si(2)–C(30)	122.7(2)	C(15)–C(16)–C(19)	112.9(5)
C(8)–Si(2)–C(25)	110.4(3)	C(17)–C(16)–C(18)	107.2(5)
C(8)–Si(2)–C(30)	103.6(3)	C(17)–C(16)–C(19)	108.5(5)
C(25)–Si(2)–C(30)	115.1(3)	C(18)–C(16)–C(19)	109.1(5)
Si(1)–C(1)–C(2)	109.4(4)	Si(1)–C(20)–C(21)	126.2(4)
Si(1)–C(1)–C(14)	107.7(4)	C(20)–C(21)–C(22)	108.2(5)
C(2)–C(1)–C(14)	108.2(4)	C(20)–C(21)–C(23)	110.5(5)
C(1)–C(2)–C(3)	122.5(6)	C(20)–C(21)–C(24)	112.9(5)
C(1)–C(2)–C(7)	117.2(5)	C(22)–C(21)–C(23)	107.3(6)
C(3)–C(2)–C(7)	120.3(6)	C(22)–C(21)–C(24)	108.7(6)
C(2)–C(3)–C(4)	119.9(7)	C(23)–C(21)–C(24)	109.0(6)
C(3)–C(4)–C(5)	120.1(7)	Si(2)–C(25)–C(26)	126.9(4)
C(4)–C(5)–C(6)	120.9(8)	C(25)–C(26)–C(27)	107.8(6)
C(5)–C(6)–C(7)	120.3(7)	C(25)–C(26)–C(28)	111.1(6)
C(2)–C(7)–C(6)	118.5(6)	C(25)–C(26)–C(29)	111.6(6)
C(2)–C(7)–C(8)	117.0(5)	C(27)–C(26)–C(28)	107.7(7)
C(6)–C(7)–C(8)	124.5(6)	C(27)–C(26)–C(29)	110.1(7)
Si(2)–C(8)–C(7)	110.6(4)	C(28)–C(26)–C(29)	108.4(6)
Si(2)–C(8)–C(9)	107.1(4)	Si(2)–C(30)–C(31)	126.4(5)
C(7)–C(8)–C(9)	108.8(5)	C(30)–C(31)–C(32)	109.2(6)
C(8)–C(9)–C(10)	123.8(5)	C(30)–C(31)–C(33)	109.4(7)
C(8)–C(9)–C(14)	117.0(5)	C(30)–C(31)–C(34)	112.5(6)
C(10)–C(9)–C(14)	119.3(5)	C(32)–C(31)–C(33)	106.6(7)
C(9)–C(10)–C(11)	120.5(6)	C(32)–C(31)–C(34)	107.3(7)
C(10)–C(11)–C(12)	120.2(6)	C(33)–C(31)–C(34)	111.6(7)

Fig. 2. NOESY spectrum of **1** in CD_2Cl_2 .

1, and interacts with two benzene rings of **1**. The mean distance between the benzene rings and the TCNE plane is 3.44 \AA , which is somewhat longer than that of the charge-transfer complex of bi(benzo[*c*]-1-isopro-

pylsilacyclopent-3-en-1-yl) with TCNE (3.31 \AA) [4b]. The dihedral angle between two *o*-xylylene planes of **1** (134.3°) is somewhat greater than that of isolated **1** (130.1°). In Fig. 6, the packing diagram of the charge-transfer complex is shown. The charge-transfer interaction between the benzene rings and TCNE is insulated by the neopentyl groups, and the charge-transfer zone and the insulator are stacked alternatively.

Fig. 3. UV spectra of **1** and **2** in hexane at room temperature.Fig. 4. Charge-transfer absorption spectra of **1** and **2** with TCNE in dichloromethane at room temperature. The concentrations of **1**, **2** and TCNE are 0.10, 0.10 and 0.013 M respectively.

2.5. Cycloreversion of 2 with transition metal chlorides

Treatment of 2 with an equimolar amount of $\text{PdCl}_2(\text{PhCN})_2$ in refluxing benzene resulted in cyclore-

version of 2 to give 1,2-dichlorotetraisopropyldisilane and anthracene almost quantitatively. The cycloreversion of 2 also occurred by $\text{PtCl}_2(\text{PhCN})_2$ or $[\text{RhCl}(\text{CO})_2]_2$, although the reactions proceeded more

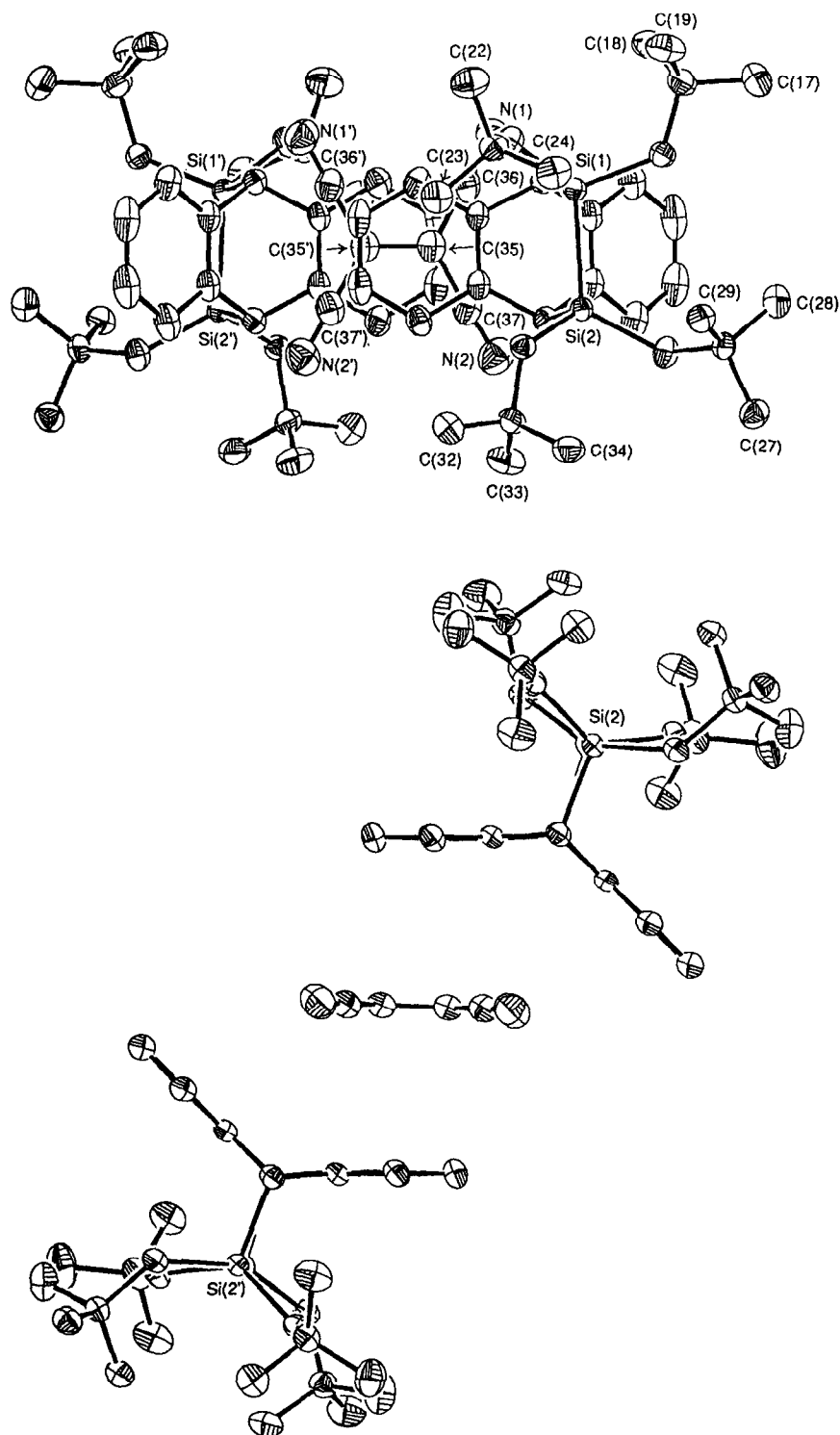
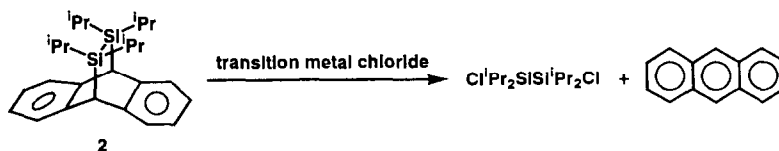


Fig. 5. Top view (top) and side view (bottom) of the molecular structure of the charge-transfer complex of 1 with TCNE. The numbering of 1 is identical with that of 1 in Fig. 1. Thermal ellipsoids are drawn at the 30% probability level.

slowly than the cycloreversion with $\text{PdCl}_2(\text{PhCN})_2$. Compound **2** did not react with transition metal chloro-

rides bearing phosphine ligands, e.g. PEt_3 or PPh_3 . The results are summarized in Table 7.



Although the reaction mechanism is not clear [11], these products are apparently derived from cleavage of the benzylic Si–C bonds of **2**. It is noted that the Si–Si bond of **2** was not cleaved in these reactions, while strained Si–Si bonds are well known to be readily

cleaved by transition metal complexes [12]. Therefore, our results provide the first example of Si–C cleavage in cyclic carbopolysilane systems by transition metal chlorides.

Table 5
Fractional atomic coordinates and equivalent isotropic thermal parameters for **1**–TCNE

Atom	x	y	z	B_{eq}^a (\AA^2)
Si(1)	0.1441(1)	0.15557(3)	0.4547(1)	3.00(3)
Si(2)	0.1325(1)	0.08909(3)	0.4541(1)	2.91(3)
C(1)	0.2076(5)	0.1604(1)	0.5524(2)	3.5(1)
C(2)	0.1131(5)	0.1410(2)	0.5899(2)	3.8(1)
C(3)	0.0305(6)	0.1600(2)	0.6263(3)	5.0(2)
C(4)	–0.0530(6)	0.1396(3)	0.6606(3)	6.3(3)
C(5)	–0.0543(6)	0.1021(3)	0.6590(3)	6.0(2)
C(6)	0.0271(6)	0.0830(2)	0.6239(3)	5.0(2)
C(7)	0.1120(5)	0.1026(2)	0.5890(2)	3.7(1)
C(8)	0.2047(5)	0.0833(1)	0.5505(2)	3.5(1)
C(9)	0.3382(5)	0.1022(1)	0.5654(2)	3.4(1)
C(10)	0.4584(6)	0.0828(2)	0.5766(3)	4.4(2)
C(11)	0.5771(6)	0.1019(2)	0.5871(3)	5.2(2)
C(12)	0.5782(6)	0.1397(2)	0.5878(3)	5.2(2)
C(13)	0.4601(6)	0.1595(2)	0.5786(3)	4.5(2)
C(14)	0.3393(5)	0.1407(1)	0.5664(2)	3.4(1)
C(15)	–0.0298(5)	0.1748(1)	0.4307(3)	4.0(1)
C(16)	–0.0709(6)	0.2158(2)	0.4273(3)	5.0(2)
C(17)	–0.2224(8)	0.2170(3)	0.4216(7)	8.2(3)
C(18)	–0.0058(9)	0.2369(2)	0.4903(4)	5.7(2)
C(19)	–0.0381(10)	0.2348(2)	0.3642(4)	6.5(2)
C(20)	0.2726(6)	0.1828(2)	0.4179(3)	4.4(2)
C(21)	0.3059(6)	0.1789(2)	0.3463(3)	4.4(1)
C(22)	0.3521(11)	0.2161(2)	0.3236(4)	6.5(3)
C(23)	0.4200(8)	0.1516(2)	0.3477(6)	7.2(3)
C(24)	0.1870(8)	0.1649(2)	0.2955(3)	5.5(2)
C(25)	–0.0340(5)	0.0647(2)	0.4443(3)	4.3(2)
C(26)	–0.1512(5)	0.0683(1)	0.3836(3)	3.7(1)
C(27)	–0.2119(7)	0.0301(2)	0.3662(4)	4.9(2)
C(28)	–0.2591(7)	0.0929(2)	0.4023(5)	6.2(2)
C(29)	–0.1065(6)	0.0839(2)	0.3211(3)	4.5(2)
C(30)	0.2509(5)	0.0685(1)	0.4020(3)	3.5(1)
C(31)	0.2735(5)	0.0268(1)	0.3907(3)	4.0(1)
C(32)	0.4011(8)	0.0229(2)	0.3620(5)	6.4(2)
C(33)	0.2861(9)	0.0046(2)	0.4561(4)	6.1(2)
C(34)	0.1620(8)	0.0105(2)	0.3382(4)	5.4(2)
C(35)	0.4327(6)	0.1240(2)	0.7451(3)	4.7(1)
C(36)	0.3617(7)	0.1580(2)	0.7406(3)	5.4(2)
C(37)	0.3611(6)	0.0899(2)	0.7401(3)	5.1(2)
N(1)	0.3053(8)	0.1853(2)	0.7381(4)	7.6(2)
N(2)	0.3042(8)	0.0629(2)	0.7368(3)	7.2(2)

^a Anisotropically refined atoms are given in the form of the equivalent isotropic displacement parameter defined as $B_{\text{eq}} = (4/3)\sum_i \beta_i \mathbf{a}_i \mathbf{a}_i$.

Table 6
Bond distances (Å) and angles (°) for 1-TCNE^a

<i>Bond distances</i>			
Si(1)–Si(2)	2.401(2)	C(13)–C(14)	1.396(8)
Si(1)–C(1)	1.951(5)	C(15)–C(16)	1.539(8)
Si(1)–C(15)	1.892(5)	C(16)–C(17)	1.540(11)
Si(1)–C(20)	1.901(6)	C(16)–C(18)	1.518(10)
Si(2)–C(8)	1.946(5)	C(16)–C(19)	1.528(11)
Si(2)–C(25)	1.900(6)	C(20)–C(21)	1.540(9)
Si(2)–C(30)	1.895(6)	C(21)–C(22)	1.523(11)
C(1)–C(2)	1.505(7)	C(21)–C(23)	1.525(11)
C(1)–C(14)	1.508(7)	C(21)–C(24)	1.523(9)
C(2)–C(3)	1.396(9)	C(25)–C(26)	1.548(7)
C(2)–C(7)	1.386(8)	C(26)–C(27)	1.526(8)
C(3)–C(4)	1.403(11)	C(26)–C(28)	1.521(10)
C(4)–C(5)	1.352(15)	C(26)–C(29)	1.520(9)
C(5)–C(6)	1.373(10)	C(30)–C(31)	1.545(7)
C(6)–C(7)	1.404(8)	C(31)–C(32)	1.533(11)
C(7)–C(8)	1.502(7)	C(31)–C(33)	1.519(10)
C(8)–C(9)	1.510(7)	C(31)–C(34)	1.521(9)
C(9)–C(10)	1.400(8)	C(35)–C(36)	1.422(10)
C(9)–C(14)	1.389(7)	C(35)–C(37)	1.426(10)
C(10)–C(11)	1.382(9)	C(35)–C(35')	1.360(9)
C(11)–C(12)	1.364(11)	C(36)–N(1)	1.140(11)
C(12)–C(13)	1.391(9)	C(37)–N(2)	1.130(11)
<i>Bond angles</i>			
Si(2)–Si(1)–C(1)	95.8(2)	C(1)–C(14)–C(13)	122.7(5)
Si(2)–Si(1)–C(15)	108.7(2)	C(9)–C(14)–C(13)	119.6(5)
Si(2)–Si(1)–C(20)	123.5(2)	Si(1)–C(15)–C(16)	127.0(4)
C(1)–Si(1)–C(15)	110.3(2)	C(15)–C(16)–C(17)	107.1(6)
C(1)–Si(1)–C(20)	102.5(2)	C(15)–C(16)–C(18)	111.7(5)
C(15)–Si(1)–C(20)	113.7(3)	C(15)–C(16)–C(19)	111.6(6)
Si(1)–Si(2)–C(8)	95.4(2)	C(17)–C(16)–C(18)	109.4(7)
Si(1)–Si(2)–C(25)	120.4(2)	C(17)–C(16)–C(19)	107.5(7)
Si(1)–Si(2)–C(30)	111.0(2)	C(18)–C(16)–C(19)	109.4(6)
C(8)–Si(2)–C(25)	102.9(2)	Si(1)–C(20)–C(21)	127.1(4)
C(8)–Si(2)–C(30)	109.8(2)	C(20)–C(21)–C(22)	109.3(6)
C(25)–Si(2)–C(30)	114.7(2)	C(20)–C(21)–C(23)	110.2(6)
Si(1)–C(1)–C(2)	109.5(3)	C(20)–C(21)–C(24)	111.3(5)
Si(1)–C(1)–C(14)	105.4(3)	C(22)–C(21)–C(23)	107.1(7)
C(2)–C(1)–C(14)	109.1(4)	C(22)–C(21)–C(24)	110.3(6)
C(1)–C(2)–C(3)	122.8(5)	C(23)–C(21)–C(24)	108.5(6)
C(1)–C(2)–C(7)	117.5(5)	Si(2)–C(25)–C(26)	126.6(4)
C(3)–C(2)–C(7)	119.6(5)	C(25)–C(26)–C(27)	109.2(5)
C(2)–C(3)–C(4)	118.8(7)	C(25)–C(26)–C(28)	110.6(5)
C(3)–C(4)–C(5)	121.2(7)	C(25)–C(26)–C(29)	111.6(5)
C(4)–C(5)–C(6)	120.6(7)	C(27)–C(26)–C(28)	107.4(5)
C(5)–C(6)–C(7)	119.7(7)	C(27)–C(26)–C(29)	108.6(5)
C(2)–C(7)–C(6)	120.0(5)	C(28)–C(26)–C(29)	109.3(5)
C(2)–C(7)–C(8)	117.8(5)	Si(2)–C(30)–C(31)	126.3(4)
C(6)–C(7)–C(8)	122.2(5)	C(30)–C(31)–C(32)	107.8(5)
Si(2)–C(8)–C(7)	107.3(3)	C(30)–C(31)–C(33)	112.2(5)
Si(2)–C(8)–C(9)	108.1(3)	C(30)–C(31)–C(34)	111.3(4)
C(7)–C(8)–C(9)	109.2(4)	C(32)–C(31)–C(33)	109.5(6)
C(8)–C(9)–C(10)	123.2(5)	C(32)–C(31)–C(34)	106.9(6)
C(8)–C(9)–C(14)	117.3(4)	C(33)–C(31)–C(34)	109.0(5)
C(10)–C(9)–C(14)	119.5(5)	C(36)–C(35)–C(37)	119.3(6)
C(9)–C(10)–C(11)	120.1(6)	C(36)–C(35)–C(35')	120.3(6)
C(10)–C(11)–C(12)	120.4(6)	C(37)–C(35)–C(35')	120.5(6)
C(11)–C(12)–C(13)	120.5(6)	C(35)–C(36)–N(1)	178.9(7)
C(12)–C(13)–C(14)	119.9(6)	C(35)–C(37)–N(2)	179.3(7)
C(1)–C(14)–C(9)	117.7(4)		

^a Primed atoms are generated by the crystallographic symmetry operator (1 – x, y, 3/2 – z).

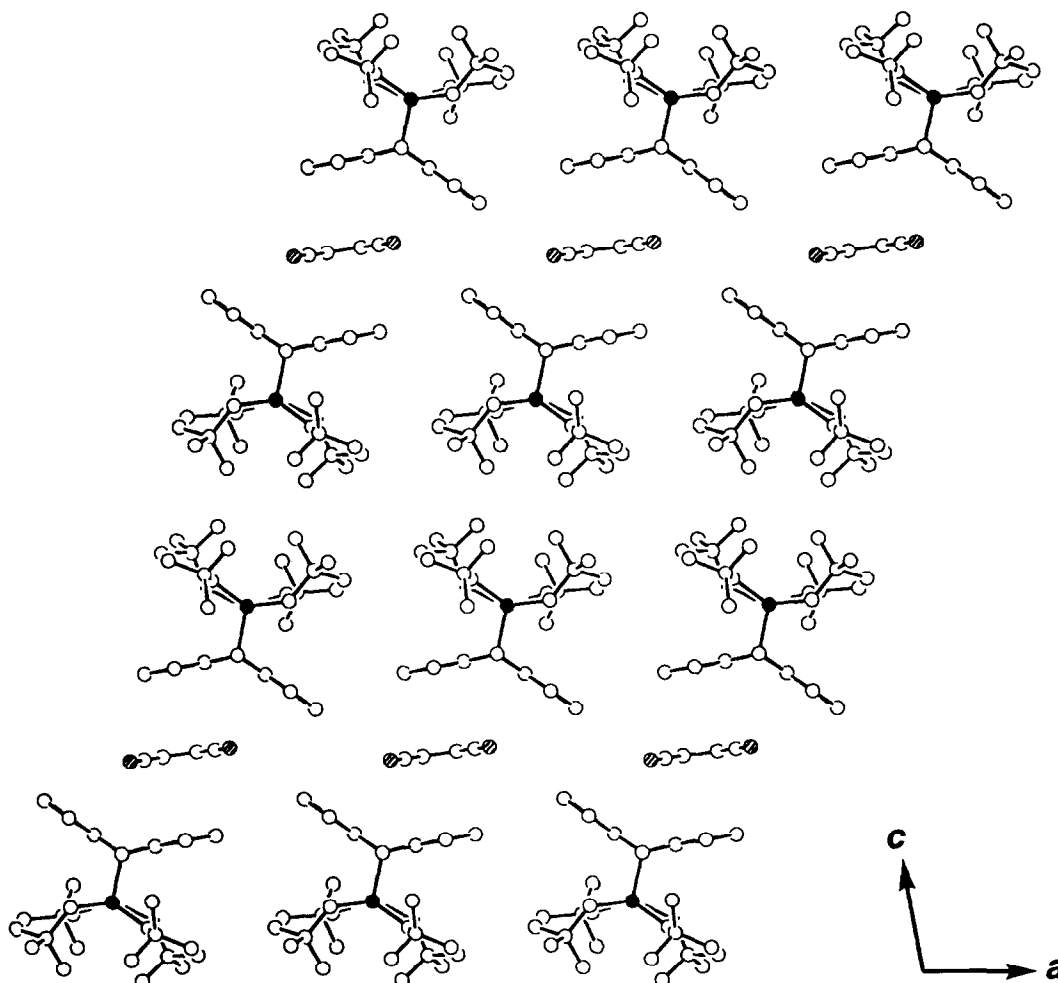


Fig. 6. Packing diagram of the charge-transfer complex of **1** and TCNE viewed along the *b* axis. The filled circles denote silicon atoms, nitrogen atoms are shaded.

3. Experimental details

All operations were carried out under a nitrogen atmosphere unless otherwise noted. Petroleum ether, benzene and hexane were distilled from lithium aluminum hydride. For reactions involving transition metal chlorides, benzene was further degassed by freeze-pump-thaw cycles just before use. Diethyl ether, tetra-

hydrofuran (THF) and DME were distilled from sodium benzophenone ketyl. Ethanol and dichloromethane were distilled. Acetonitrile was distilled from calcium hydride. Dibenzo[*b,e*]-7,7,8,8-tetraisopropyl-7,8-disilabicyclo[2.2.2]octa-2,5-diene (**2**) [5] and neopentyl chloride [13] were prepared by published procedures. Lithium (Nacalai Tesque) and lithium dispersion (Aldrich, 30% in mineral oil) were purchased. Hydrogen chloride was

Table 7
Cycloreversion of **2** with transition metal chlorides ^a

Transition metal chloride	Reaction time (h)	Conversion of 2 (%) ^b	Conversion yield (%) ^b	
			Cl ¹ Pr ₂ SiSi ¹ Pr ₂ Cl	Anthracene
PdCl ₂ (PhCN) ₂	39	85	99	99
PdCl ₂ (PEt ₃) ₂	36	0	0	0
PtCl ₂ (PhCN) ₂	110	17	99	99
<i>cis</i> -PtCl ₂ (PEt ₃) ₂	20	0	0	0
[RhC(CO) ₂] ₂	62	75	56	72
RhCl(PPh ₃) ₃	74	0	0	0

^a Reaction conditions: **2**/transition metal chloride = 1/1 in benzene at reflux temperature.

^b Determined by GLC using *n*-C₂₂H₄₆ as an internal standard.

passed through sulfuric acid before use. Aluminum chloride (extra pure grade) was purchased from Wako Pure Chemical Industries, Ltd. Anthracene was recrystallized from THF. TCNE was sublimed under reduced pressure. $\text{PdCl}_2(\text{PhCN})_2$ [14], $\text{PdCl}_2(\text{PEt}_3)_2$ [15], $\text{PtCl}_2(\text{PhCN})_2$ [16], *cis*- $\text{PtCl}_2(\text{PEt}_3)_2$ [17] and $\text{RhCl}(\text{PPh}_3)_3$ [18] were prepared by published procedures. $[\text{RhCl}(\text{CO})_2]_2$ (Aldrich) was used without further purification.

^1H , ^{13}C and ^{29}Si NMR spectra were obtained with JEOL JNM-A500 and Varian Gemini-200 spectrometers. IR spectra were recorded on a JASCO A-102 spectrometer. UV-visible spectra were obtained with a JASCO Ubest-50 spectrophotometer. Mass spectra were recorded on a JEOL JMS-DX302 mass spectrometer. Elemental analyses were performed by the Institute of Physical and Chemical Research. Oxidation potentials were measured by cyclic voltammetry in acetonitrile containing 0.1 M tetrabutylammonium perchlorate by using a saturated calomel electrode (SCE) as a reference. Quantitative GLC analysis was performed on an Ohkura Model-103 gas chromatograph using a 1 m column packed with 10% Silicone KF-96 on Celite 545 SK.

3.1. Preparation of neopentyl lithium in petroleum ether

Neopentyl lithium in petroleum ether was prepared by a modified procedure of the previously reported method [19]. A solution of neopentyl chloride (45 g, 0.42 mol) in petroleum ether (100 ml) was added to finely cut lithium (8.8 g, 1.3 mol) in petroleum ether (100 ml) at room temperature under ultrasonic irradiation. The mixture was stirred for 10 h under ultrasonic irradiation and reflux to give a solution of neopentyl lithium. The concentration of the solution was determined by titration with 2-butanol using 1,10-phenanthroline as an indicator (1.18 M, 70%) [20].

3.2. Synthesis of chlorodineopentylphenylsilane

A solution of neopentyl lithium in petroleum ether (1.18 M, 280 ml) was added dropwise to a solution of trichlorophenylsilane (28.4 g, 0.134 mol) in diethyl ether (230 ml) at 0°C. The mixture was stirred for 12 h at room temperature. The precipitate was removed by filtration and the filtrate was hydrolyzed. The organic layer was washed with dilute aqueous acetic acid and aqueous sodium chloride, and dried over anhydrous magnesium sulfate. The solvents were evaporated, and chlorodineopentylphenylsilane (33.5 g, 88%) was distilled under reduced pressure. B.p. 85°C/2 mmHg. ^1H NMR (CDCl_3): δ 0.94 (s, 18H), 1.20 (d, 2H, $J = 15.1$ Hz), 1.24 (d, 2H, $J = 15.1$ Hz), 7.35–7.40 (m, 3H), 7.67–7.69 (m, 2H). ^{13}C NMR (CDCl_3): δ 31.4, 32.9, 34.8, 127.8, 129.7, 133.8, 137.0. ^{29}Si NMR (CDCl_3): δ

16.1. IR (NaCl , cm^{-1}): 3080, 2960, 1467, 1429, 1364, 1260, 1236, 1112. MS: m/z 282 (2, M^+), 267 (24), 211 (64), 155 (100). HRMS. Anal. Found: 282.1558. $\text{C}_{16}\text{H}_{27}\text{ClSi}$. Calc.: 282.1570.

3.3. Synthesis of 1,1,2,2-tetraneopentyl-1,2-diphenyldisilane

A mixture of chlorodineopentylphenylsilane (28.4 g, 0.100 mol), finely cut lithium (2.08 g, 0.300 mol), THF (100 ml) and benzene (100 ml) was stirred for 2 h at room temperature under ultrasonic irradiation. Unreacted lithium was removed by filtration, and the filtrate was hydrolyzed. The organic layer was washed with dilute aqueous acetic acid and aqueous sodium chloride, and dried over anhydrous magnesium sulfate. The solvents were evaporated, and the residue was recrystallized from ethanol to give 1,1,2,2-tetraneopentyl-1,2-diphenyldisilane (21.0 g, 85%) as colorless crystals. M.p. 185–188°C. ^1H NMR (CDCl_3): δ 0.83 (s, 36H), 1.39 (d, 4H, $J = 14.8$ Hz), 1.47 (d, 4H, $J = 14.8$ Hz), 7.25–7.27 (m, 6H), 7.58–7.60 (m, 4H). ^{13}C NMR (CDCl_3): δ 30.0, 32.0, 33.8, 127.2, 128.1, 135.7, 139.4. ^{29}Si NMR (CDCl_3): δ -24.3. IR (KBr, cm^{-1}): 3080, 2950, 1460, 1425, 1359, 1225, 1155, 1095, 765, 700. MS: m/z 494 (0.6, M^+), 423 (3), 247 (61), 191 (46), 135 (100). Anal. Found: C, 77.73; H, 10.97. $\text{C}_{32}\text{H}_{54}\text{Si}_2$. Calc.: C, 77.65; H, 11.00%.

3.4. Synthesis of 1,2-dichloro-1,1,2,2-tetraneopentyl-disilane

Hydrogen chloride was passed through a mixture of 1,1,2,2-tetraneopentyl-1,2-diphenyldisilane (19.1 g, 38.6 mmol), aluminum chloride (5.18 g, 38.8 mmol) and benzene (150 ml) for 15 min at room temperature. After removing the solvents under reduced pressure, hexane (150 ml) was added and the mixture was filtered. The filtrate was evaporated, and the residue was recrystallized from acetonitrile to give 1,2-dichloro-1,1,2,2-tetraneopentyl-disilane (13.3 g, 84%) as colorless crystals. M.p. 72–73°C. ^1H NMR (CDCl_3): δ 1.10 (s, 36H), 1.22 (d, 4H, $J = 15.0$ Hz), 1.34 (d, 4H, $J = 15.0$ Hz). ^{13}C NMR (CDCl_3): δ 32.0, 33.2, 34.2. ^{29}Si NMR (CDCl_3): δ 15.2. IR (KBr, cm^{-1}): 2940, 1472, 1355, 1228, 765, 670. MS: m/z 410 (2, M^+), 170 (51), 149 (62), 99 (51), 93 (100), 73 (94). Anal. Found: C, 58.37; H, 10.83. $\text{C}_{20}\text{H}_{44}\text{Cl}_2\text{Si}_2$. Calc.: C, 58.35; H, 10.77%.

3.5. Synthesis of dibenzo[*b,e*]-7,7,8,8-tetraneopentyl-7,8-disilabicyclo[2.2.2]octa-2,5-diene (1)

A solution of lithium anthracenide was prepared by the treatment of anthracene (5.00 g, 28.1 mmol) with lithium dispersion (30% in mineral oil, 0.56 g) in DME (60 ml) at room temperature under an argon atmo-

sphere. To this was added a solution of 1,2-dichloro-1,1,2,2-tetraepentylidisilane (5.00 g, 12.1 mmol) in DME (50 ml). The mixture was stirred for 1 day at room temperature. After hydrolysis, the solvent was evaporated. Diethyl ether (50 ml) was added to the residue and insoluble materials were filtered. The filtrate was evaporated, and the residue was recrystallized from ethanol to give **1** as colorless crystals (3.42 g, 54%). M.p. 179–180°C. ¹H NMR (CD₂Cl₂): δ 0.88 (d, 4H, *J* = 15.3 Hz), 0.99 (d, 4H, *J* = 15.3 Hz), 1.11 (s, 36H), 4.13 (s, 2H), 7.12 (dd, 4H, *J* = 5.5, 3.4 Hz), 7.23 (dd, 4H, *J* = 5.5, 3.4 Hz). ¹³C NMR (CD₂Cl₂): δ 30.1, 31.5, 34.1, 44.0, 124.9, 126.8, 139.8. ²⁹Si NMR (CD₂Cl₂): δ -24.6. IR (KBr, cm⁻¹): 3065, 2947, 1464, 1361, 1228, 1064, 782, 764. UV (λ_{max} in hexane) 275 (ε 3000), 282 nm (2700). MS: *m/z* 518 (2, M⁺), 447(5), 340 (100). HRMS. Anal. Found: 518.3768. C₃₄H₅₄Si₂. Calc.: 518.3764.

3.6. Isolation of the charge-transfer complex of **1** with TCNE

Compound **1** (100 mg, 0.193 mmol) and TCNE (12 mg, 0.094 mmol) were dissolved in dichloromethane (1 ml). The resulting green solution was allowed to stand in air at room temperature. Slow evaporation of the solvent provided the charge-transfer complex of **1**-TCNE (112 mg, 100%) as dark green crystals. M.p. 174–175°C (decomposed). IR (KBr, cm⁻¹): 3065, 3023, 2947, 2250 (ν C≡N), 1464, 1361, 1228, 1064, 782, 764. Anal. Found: C, 75.61; H, 9.32; N, 4.88. C₇₄H₁₀₈N₄Si₄. Calc.: C, 76.23; H, 9.34; N, 4.80%.

3.7. X-ray crystallographic analysis of **1** and the charge-transfer complex of **1** with TCNE

Colorless crystals of **1** were obtained from a methanol solution by slow evaporation. Dark green crystals of the charge-transfer complex of **1** with TCNE were grown from a dichloromethane solution of **1** and TCNE (2:1) by slow evaporation. These crystal specimens were sealed in glass capillaries and used for data collection on an Enraf-Nonius CAD-4 diffractometer using graphite-monochromated Cu Kα radiation. Cell parameters were refined by the least-squares method using 24 reflections with 44 < 2θ < 84° in the case of **1** and 25 reflections with 19 < 2θ < 31° in the case of the **1**-TCNE complex. Intensity data were collected in the range 7 < 2θ < 130° by the ω-θ scan technique (**1**) and in the range 6 < 2θ < 120° by the ω-2θ scan technique (**1**-TCNE) at room temperature. Three standard reflections were measured after every hour, showing essentially no decay. The data were corrected for Lorentz and polarization effects. An empirical absorption correction based on a ψ scan was also applied. The structure was solved by direct methods using MULTAN80 [21] in the

case of **1** and MULTAN78 [22] in the case of the **1**-TCNE complex. Non-hydrogen atoms were refined by the full-matrix least-squares method with anisotropic thermal parameters using UNICSIII [23]. In the case of **1**, 49 hydrogen atoms were located by difference Fourier synthesis and the remaining hydrogen atoms were located at calculated positions. All hydrogen atoms were not refined. In the case of the **1**-TCNE complex, all hydrogen atoms were located by difference Fourier synthesis and refined isotropically. Atomic scattering factors were taken from Ref. [24]. All calculations were carried out on a FACOM M-380 computer. Details of crystal data, data collection and refinement are listed in Table 2.

3.8. Cycloreversion of **2** with transition metal chlorides

Typical procedures are described for the reaction of **2** with PdCl₂(PhCN)₂. A solution of **2** (25 mg, 0.061 mmol) and PdCl₂(PhCN)₂ (24 mg, 0.062 mmol) in benzene (2.5 ml) was refluxed for 39 h. As the reaction proceeded, a black solid was deposited on the wall of the reaction vessel. GLC analysis of the resulting mixture showed that 85% of **2** was consumed to give 1,2-dichloro-1,1,2,2-tetraisopropylidisilane and anthracene almost quantitatively.

Acknowledgments

This work was supported in part by Grants-in-Aid for Scientific Research (Priority Area of Reactive Organometallics No. 05236206 and Organic Unusual Valency No. 03233105) from the Ministry of Education, Science and Culture, Japan. We thank Shin-etsu Chemical Co., Ltd., Toshiba Silicone Co., Ltd. and Yuki Gosei Kogyo Co., Ltd. for financial support.

References and notes

- [1] For reviews: (a) G. Raabe and J. Michl, *Chem. Rev.*, 85 (1985) 419; (b) R. West, *Angew. Chem., Int. Ed. Engl.*, 26 (1987) 1201; (c) G. Raabe and J. Michl, in S. Patai and Z. Rappaport (eds.), *The Chemistry of Organic Silicon Compounds*, Wiley, Chichester, 1989, Chapter 17.
- [2] (a) D.N. Roark and G.J.D. Peddle, *J. Am. Chem. Soc.*, 94 (1972) 5837; (b) T.J. Barton and J.A. Kilgour, *J. Am. Chem. Soc.*, 98 (1976) 7231; (c) T.J. Barton and J.A. Kilgour, *J. Am. Chem. Soc.*, 98 (1976) 7746; (d) H. Sakurai, Y. Nakadaira and T. Kobayashi, *J. Am. Chem. Soc.*, 101 (1979) 487; (e) J.D. Rich, T.J. Drahnak, R. West and J. Michl, *J. Organomet. Chem.*, 212 (1981) C1; (f) Y. Nakadaira, T. Otsuka and H. Sakurai, *Tetrahedron Lett.*, 22 (1981) 2417; (g) S. Masamune, S. Murakami and H. Tobita, *Organometallics*, 2 (1983) 1464; (h) H. Sakurai, Y. Nakadaira and H. Sakaba, *Organometallics*, 2 (1983) 1484; (i) A. Sekiguchi, I. Maruki, K. Ebata, C. Kabuto and H. Sakurai, *J. Chem. Soc., Chem. Commun.*, (1991) 341.

- [3] Y. Nakadaira, Y. Gomi, H. Hosoe, S. Kyushin, M. Kako, K. Hatakenaka and M. Ohashi, *Bull. Chem. Soc. Jpn.*, **66** (1993) 344.
- [4] (a) S. Kyushin, Y. Izumi, S. Tsunakawa and H. Matsumoto, *Chem. Lett.*, (1992) 1393; (b) S. Kyushin, M. Ikarugi, S. Tsunakawa, Y. Izumi, M. Miyake, M. Sato, H. Matsumoto and M. Goto, *J. Organomet. Chem.*, **473** (1994) 19.
- [5] H. Matsumoto, T. Arai, H. Watanabe and Y. Nagai, *J. Chem. Soc., Chem. Commun.*, (1984) 724.
- [6] (a) T.G. Traylor, W. Hanstein, H.J. Berwin, N.A. Clinton and R.S. Brown, *J. Am. Chem. Soc.*, **93** (1971) 5715; (b) H. Sakurai, S. Tasaka and M. Kira, *J. Am. Chem. Soc.*, **94** (1972) 9285.
- [7] It has been reported that charge-transfer bands of silyl-substituted benzene–TCNE complexes are well simulated by skewed Gaussian lines [25]. However, the charge-transfer bands of **1** and **2** with TCNE could not be simulated by two skewed Gaussian lines because the width of the higher-energy band is significantly larger than that of the lower-energy band. It seems that the charge-transfer bands consist of more than two components.
- [8] For a review: V.F. Traven and S.Y. Shapakin, *Adv. Organomet. Chem.*, **34** (1992) 149.
- [9] (a) H. Bock and H. Alt, *Angew. Chem., Int. Ed. Engl.*, **6** (1967) 942; (b) H. Bock, H. Seidl and M. Fochler, *Chem. Ber.*, **101** (1968) 2815; (c) W. Hanstein, H.J. Berwin and T.G. Traylor, *J. Am. Chem. Soc.*, **92** (1970) 829; (d) H. Bock and H. Alt, *J. Am. Chem. Soc.*, **92** (1970) 1569; (e) C.G. Pitt, *J. Organomet. Chem.*, **23** (1970) C35; (f) H. Sakurai, M. Kira and M. Ochiai, *Chem. Lett.*, (1972) 87; (g) V.F. Traven and R. West, *J. Am. Chem. Soc.*, **95** (1973) 6824; (h) H. Sakurai, M. Kira and T. Uchida, *J. Am. Chem. Soc.*, **95** (1973) 6826; (i) H. Sakurai and M. Kira, *J. Am. Chem. Soc.*, **96** (1974) 791; (j) H. Sakurai, K. Sakamoto and M. Kira, *Chem. Lett.*, (1984) 1213; (k) H. Sakurai, M. Ichinose, M. Kira and T.G. Traylor, *Chem. Lett.*, (1984) 1383; (l) M. Kira, K. Takeuchi, C. Kabuto and H. Sakurai, *Chem. Lett.*, (1988) 353.
- [10] S. Kyushin, Y. Ohkura, Y. Nakadaira, M. Ohashi, M. Yasui, M. Matsui and F. Iwasaki, *Chem. Lett.*, (1991) 883.
- [11] A referee pointed out the possibility of the participation of electron transfer in the cycloreversion. We think that electron transfer is probable as reported in the cycloreversion of 2,3-disilabicyclo[2.2.2]octa-5,7-diene derivatives via photo-induced electron transfer [3].
- [12] (a) H. Sakurai, Y. Kamiyama and Y. Nakadaira, *J. Am. Chem. Soc.*, **97** (1975) 931; (b) H. Sakurai, Y. Kamiyama and Y. Nakadaira, *Chem. Lett.*, (1975) 887; (c) C.W. Carlson and R. West, *Organometallics*, **2** (1983) 1801; (d) A. Schäfer, M. Weidenbruch and S. Pohl, *J. Organomet. Chem.*, **282** (1985) 305; (e) M. Ishikawa, S. Okazaki, A. Naka and H. Sakamoto, *Organometallics*, **11** (1992) 4135.
- [13] D.R. Hepburn and H.R. Hudson, *J. Chem. Soc., Perkin Trans. I*, (1976) 754.
- [14] J.R. Doyle, P.E. Slade and H.B. Jonassen, *Inorg. Synth.*, **6** (1960) 216.
- [15] J.M. Jenkins and B.L. Shaw, *J. Chem. Soc., Sect. A*, (1966) 770.
- [16] K.A. Hofmann and G. Bugge, *Ber.*, **40** (1907) 1772.
- [17] G.W. Parshall, *Inorg. Synth.*, **12** (1970) 27.
- [18] J.A. Osborn and G. Wilkinson, *Inorg. Synth.*, **10** (1967) 67.
- [19] R.R. Schrock and J.D. Fellmann, *J. Am. Chem. Soc.*, **100** (1978) 3359.
- [20] S.C. Watson and J.F. Eastham, *J. Organomet. Chem.*, **9** (1967) 165.
- [21] P. Main, S.J. Fiske, S.E. Hull, L. Lessinger, G. Germain, J.-P. Declercq and M.M. Woolfson, *MULTAN80, A System of Computer Programs for the Automatic Solution of Crystal Structures from X-ray Diffraction Data*, Universities of York, UK and Louvain, Belgium, 1980.
- [22] P. Main, S.E. Hull, L. Lessinger, G. Germain, J.-P. Declercq and M.M. Woolfson, *MULTAN78, A System of Computer Programs for the Automatic Solution of Crystal Structures from X-ray Diffraction Data*, Universities of York, UK and Louvain, Belgium, 1978.
- [23] T. Sakurai and K. Kobayashi, *Rikagaku Kenkyusho Hokoku*, **55** (1979) 69.
- [24] D.T. Cromer and J.T. Waber, *International Tables for X-ray Crystallography*, Vol. IV, Kynoch, Birmingham, UK, 1974, Table 2.3.1.
- [25] H. Sakurai and M. Kira, *J. Am. Chem. Soc.*, **97** (1975) 4879.